Kinetic Characterization of Recombinant Human Acidic Mammalian Chitinase

Yi-Te Chou,[‡] Shihua Yao,[‡] Robert Czerwinski,[‡] Margaret Fleming,[§] Rustem Krykbaev,[§] Dejun Xuan,[§] Huanfang Zhou,[§] Jonathan Brooks,[§] Lori Fitz,[§] James Strand,[‡] Eleonora Presman,[‡] Laura Lin,[‡] Ann Aulabaugh,[‡] and Xinyi Huang*,[‡]

Departments of Chemical and Screening Sciences and of Inflammation, Wyeth Research, 500 Arcola Road, Collegeville, Pennsylvania 19426

Received December 20, 2005; Revised Manuscript Received February 21, 2006

ABSTRACT: Human acidic mammalian chitinase (AMCase), a member of the family 18 glycosyl hydrolases, is one of the important proteins involved in Th2-mediated inflammation and has been implicated in asthma and allergic diseases. Inhibition of AMCase results in decreased airway inflammation and airway hyperresponsiveness in a mouse asthma model, suggesting that the AMCase activity is a part of the mechanism of Th2 cytokine-driven inflammatory response in asthma. In this paper, we report the first detailed kinetic characterization of recombinant human AMCase. In contrast with mouse AMCase that has been reported to have a major pH optimum at 2 and a secondary pH optimum around 3−6, human AMCase has only one pH optimum for k_{cat}/K_m between pH 4 and 5. Steady state kinetics shows that human AMCase has "low" intrinsic transglycosidase activity, which leads to the observation of apparent substrate inhibition. This slow transglycosylation may provide a mechanism in vivo for feedback regulation of the chitinase activity of human AMCase. HPLC characterization of cleavage of chitooligosaccharides (4−6-mers) suggests that human AMCase prefers the β anomer of chitooligosaccharides as substrate. Human AMCase also appears to cleave chitooligosaccharides from the nonreducing end primarily by disaccharide units. Ionic strength modulates the enzymatic activity and substrate cleavage pattern of human AMCase against fluorogenic substrates, chitobiose-4-methylumbelliferyl and chitotriose-4-methylumbelliferyl, and enhances activity against chitooligosaccharides. The physiological implications of these results are discussed.

Chitinases catalyze the hydrolysis of chitin, a polysaccharide of β-1,4-linked *N*-acetylglucosamine (GlcNAc).[1] Chitin is a major constituent of the cell wall of fungi and the exoskeleton of insects and crustaceans. Chitin has so far not been found in mammals. Chitinases have been identified in a variety of organisms from bacteria and fungi to plants and vertebrates (*1*). Chitinases belong to families 18 and 19 of glycosyl hydrolases that have distinct enzyme structures and catalytic mechanisms (*2*). The catalytic domains of the family 18 chitinases have an $(\alpha/\beta)_8$-barrel fold. Family 18 chitinases are proposed to utilize the substrate-assisted catalytic mechanism as illustrated in Scheme 1. The acetyl group of the (−1) GlcNAc unit of the bound chitooligosaccharide makes a nucleophilic attack on C-1 to yield an oxazolinium intermediate. Subsequent general base catalysis affords the product with retention of configuration (*3*−*5*). In contrast, family 19 chitinases show a lysozyme-like fold that consists mostly of α-helices and generally are thought to use a general acid−base mechanism, which generates the product with an inverted configuration (*5*−*7*).

Chitinases can also be classified as endo-chitinases and exo-chitinases. Endo-chitinases cleave chitin randomly at internal sites, generating multimers of GlcNAc, such as chitotetraose, chitotriose, and chitobiose. Exo-chitinases catalyze the hydrolysis of chitin progressively from either the nonreducing end or the reducing end to produce chitobiose or chitotriose, respectively. Some exo-chitinases are reported to release monomers of GlcNAc by hydrolyzing chitin from the reducing end (*1*).

Acidic mammalian chitinase (AMCase) and chitotriosidase are two of a few human chitinases that have been documented recently, although chitin and chitin synthases have not been found in mammals (*8*−*10*). Both AMCase and chitotriosidase are members of the family 18 glycosyl hydrolases. Chitotriosidase is expressed by lipid-laden tissue macrophages in humans (*10*, *11*). Human AMCase is highly expressed in the stomach and at a lower level in the lung. The endogenous substrates for human AMCase and physiological functions of human AMCase are currently unknown. AMCase is characterized by an acidic isoelectric point, which differs from the neutral/basic pI of chitotriosidase. Mouse AMCase is reported to have a major pH optimum around 2 and a secondary optimum around 3−6 and is extremely acid stable (*9*). The level of sequence identity between the human AMCase and the mouse AMCase is 82%. Human AMCase is a 50 kDa enzyme that contains a C-terminal chitin binding domain, an N-terminal catalytic domain (39 kDa), and a short hinge region (*12*). As in all other family 18 chitinases, the core catalytic motif (DXXDXDXE) is conserved in AMCase.

* To whom correspondence should be addressed. E-mail: huangx@wyeth.com. Phone: (484) 865-3805. Fax: (484) 865-9345.
[‡] Department of Chemical and Screening Sciences.
[§] Department of Inflammation.

[1] Abbreviations: 4-MU, 4-methylumbelliferone; AMCase, acidic mammalian chitinase; CD, circular dichroism; chitobiose-4MU, 4-methylumbelliferyl β-*N*,*N*′-diacetylchitobioside; DMSO, dimethyl sulfoxide; GlcNAc, 2-acetamido-2-deoxy-D-glucopyranose; $(GlcNAc)_n$, β-1,4-linked oligosaccharide of GlcNAc with a polymerization degree of *n*; SEC−MALLS, size-exclusion chromatography and multiangle light scattering.

10.1021/bi0525977 CCC: $33.50
Published on Web 03/17/2006

Scheme 1: Substrate-Assisted Catalytic Mechanism

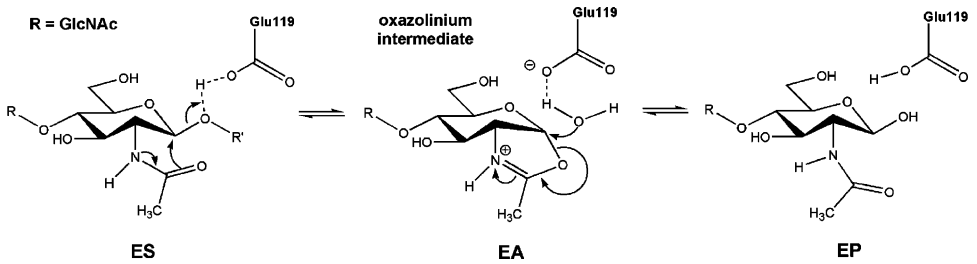

Recently, Zhu et al. (*13*) demonstrated that the expression of AMCase by airway epithelia and pulmonary macrophages is dramatically upregulated both in a mouse model of asthma and in allergic asthma in human. The authors also showed that AMCase is critical to Th2-mediated inflammation through an IL-13-dependent mechanism, and inhibition of AMCase with either an antibody or a chitinase inhibitor decreases airway inflammation and airway hyper-responsiveness (*13*). Thus, AMCase is potentially a novel target for anti-inflammatory therapy in Th2-mediated diseases such as asthma (*14*). Although the exact mechanism by which AMCase regulates Th2-driven inflammation in asthma is unknown, the importance of AMCase activity is illustrated by the fact that inhibition of AMCase by allosamidin decreases bronchoalveolar lavage and parenchymal inflammation (*13*).

A detailed kinetic characterization of human AMCase has not been published and would certainly help in our understanding of the role of AMCase in inflammation and in the design of specific and potent inhibitors of AMCase. Several studies have shown that the level and duration of activated Ca^{2+}-dependent chloride conductance were increased significantly when human bronchial epithelial cells were treated with Th2 cytokines, IL-13 or IL-4 (*15*, *16*). A separate study reported the acidification of endogenous airway in acute asthma patients (*17*). In the study presented here, we have characterized the kinetic mechanism and substrate cleavage patterns of human AMCase and also evaluated effects on the chitinolytic activity of human AMCase by pH and ionic strength. We have shown that human AMCase has low transglycosylation activity, which leads to the observation of apparent substrate inhibition and may also provide a mechanism in vivo for feedback regulation of the chitinase activity of human AMCase. We have also found that the pH optimum of human AMCase is ~4−5, and the AMCase activity is significantly enhanced in a high-salt environment, suggesting that AMCase activity in vivo is modulated by both pH and ionic strength.

MATERIALS AND METHODS

Reagents. Unless specifically mentioned, standard laboratory reagents were purchased from Sigma, Aldrich, Research Organics, or EMD.

AMCase Human Cloning and CHO Cell Development. Human stomach polyA+ RNA was purchased from BD Biosciences and used as a template in RT-PCRs (one-step RT-PCR kit, Qiagen) to obtain a DNA fragment containing the full-length AMCase sequence. Primer sequences were designed on the basis of GenBank accession number AF290004. attB recombination sequences were included for gateway cloning, and a coding sequence for C-terminal six-histidine tag fusion was included for purification purposes. The forward primer was ggggacaagtttgtacaaaaaagcaggctcgaaggagatagaaccatgacaaagcttattctcctcacaggtcttg, and the reverse primer was ggggaccactttgtacaagaaagctgggtcctagtgatggtgatggtgatgggagcctgcccagttgcagcaatcacagct. The PCR product was cloned into pTMED vector (Wyeth Research) for CMV promoter-driven expression of AMCase in a CHO stable cell line. The stably transfected AMCase CHO cell line was maintained in alpha medium (10% heat-inactivated and dialyzed FBS, 2 mM glutamine, 100 units/mL penicillin, 100 μg/mL streptomycin, 2.5 μg/mL fungizone, and 200 nM methotrexate).

AMCase Preparation. Full-length AMCase was purified from serum-free CHO conditioned medium using Ni−NTA Superflow resin (Qiagen Inc., Valencia, CA). Medium (1 L) was applied batch-wise to 6 mL of Ni−NTA resin at 4 °C within 1 h. Unbound proteins were washed away using the wash buffer [50 mM Tris (pH 8.0), 0.3 M NaCl, and 10 mM imidazole]. AMCase was then eluted using the wash buffer with 200 mM imidazole. AMCase was further purified on a 1.5 mL polypropyl aspartamide (PPA) HIC resin (The Nest Group Inc., Southborough, MA) by eluting with 50 mM Tris (pH 8.0) and 1.0 M ammonium sulfate, followed by Superdex-200 (Amersham Biosciences Inc., Piscataway, NJ) gel-filtration chromatography in 25 mM Tris (pH 8.0) and 0.4 M NaCl.

Enzyme Assays. AMCase chitinolytic activity was determined by using fluorogenic substrates 4-methylumbelliferyl β-*N*,*N*′-diacetylchitobioside (chitobiose-4MU) and 4-methylumbelliferyl β-*N*,*N*′,*N*″-triacetylchitiotrioside (chitotriose-4MU), and monitored on a Molecular Devices (Sunnyvale, CA) SpectraMax Gemini XS fluorescence plate reader with excitation at 320 nm and emission at 455 nm. Reactions were typically monitored continuously for 40 min, with less than 10% substrate conversion. Standard assays were performed in triplicate at 25 °C in 100 mM sodium citrate/citric acid, 200 mM sodium phosphate (pH 5.0), 0.005% Brij-35, and 1% DMSO. Because of the solubility issue, stock solutions of substrates were prepared in 100% DMSO and diluted to desired percentages of DMSO in the reaction buffer before reactions. The solubility of substrate in the reaction buffer was confirmed with a Nephelometer (Nephelostar Galaxy, BMG Labtech, Inc., Durham, NC). The concentration of the fluorescent 4-methylumbelliferone (4MU) product was converted from RFU using a 4MU standard curve. The velocities determined from the progress curves (the steady state rates in the case of biphasic curves) at various substrate concentrations were fit to eq 1 to determine apparent K_m and k_{cat} values using Prism (Graph Pad Software Inc., San Diego, CA).

$$v = k_{cat}ES/(S + K_m) \quad (1)$$

For the pH−activity profile, reaction buffers were prepared by mixing a sodium citrate/citric acid solution at a desired pH value and a monobasic sodium phosphate/dibasic sodium phosphate solution at the same pH value to give a buffer of 100 mM citrate and 200 mM phosphate at the desired pH value without additional pH adjustment with concentrated HCl or NaOH. Assays at various concentrations of chitobiose-4MU and chitotriose-4MU were monitored at different pHs. The k_{cat}/K_m value at each pH was calculated from the linear section of the Michaelis−Menten plot. For ionic strength experiments, assays under low-salt conditions were performed at 25 °C in 10 mM sodium citrate/citric acid, 20 mM sodium phosphate (pH 5.0), 0.005% Brij-35, and 1% DMSO. For assays under high-salt conditions, concentrated salt solutions were added to give desired high-salt buffers while the pH was maintained at 5.0 with additional HCl or NaOH, if pH was perturbed due to introduction of high salt.

Indirect Transglycosylation Assay. The standard enzyme assay using chitobiose-4MU as a substrate was modified to indirectly assess the transglycosylation activity of AMCase. The assay mixture contained chitobiose-4MU (25, 12.5, and 6.25 μM), 1 nM AMCase, and various concentrations of chitotriose (0−1000 μM). The assay was performed in triplicate at 25 °C in 100 mM sodium citrate/citric acid, 200 mM sodium phosphate (pH 5.0), 0.005% Brij-35, and 1% DMSO. The hydrolysis product 4MU was monitored fluorometrically as in the fluorogenic assay described above. In separate control experiments (fluorogenic assay and HPLC analysis), chitotriose or GlcNAc-4MU by itself was shown not to be a substrate of AMCase.

HPLC Analysis of Chitooligosaccharide Anomeric Hydrolysis Products. The analysis of anomeric forms of hydrolysis products from *N*-acetylchitooligosaccharides $(GlcNAc)_{4-6}$ was achieved by HPLC, and the cleavage pattern was assessed from the anomer formation, using a method similar to that of Arakane et al. (*18*). The enzymatic reactions were performed at 25 °C using 2 nM AMCase and 50 μM substrates in 45 mM sodium phosphate (pH 5.0). After incubation for a given period, reaction mixtures were rapidly cooled to 4 °C and immediately analyzed by Agilent 1100 HPLC. Hydrolysis products were separated on a TSKgel Amide-80 analytical column with a 78 to 72% acetonitrile/H_2O gradient over 60 min at a flow rate of 0.8 mL/min. Elution was monitored by a diode array detector with absorbance at 210 nm. The chitooligosaccharide concentration was converted from A_{210} using standard curves of $(GlcNAc)_{2-6}$. The same HPLC method was used to assess the effect of ionic strength on the AMCase reaction using chitooligosaccharides as the substrate. Data presented here were typically HPLC analysis of a single experiment and converted using triplicate standard curves. Selected HPLC analyses were performed in duplicate or triplicate. The observed errors were within 10%.

HPLC Analysis of Hydrolysis/Transglycosylation Products. AMCase reactions using chitobiose-4MU or chitotriose-4MU as the substrate were carried out under the same conditions that were used for the fluorogenic assay. After incubation for a given period, the enzymatic reactions were terminated by addition of excess 0.3 M glycine/NaOH (pH 10.3) and the mixtures analyzed by Agilent 1100 HPLC. The hydrolysis/transglycosylation products were separated on a YMC ODS-A C18 reverse-phase analytical column with a 5 to 15% acetonitrile/H_2O gradient containing 0.1% TFA over 60 min. Elution was monitored with excitation at 320 nm and emission at 455 nm by a fluorescence detector, and by a diode array detector with absorbance at 210 nm. HPLC fractions were collected and identified by a LCQ DECA XP ion trap mass spectrometer (ThermoFinnigan, San Jose, CA) and/or a Voyager DE-STR time-of-flight mass spectrometer (Applied Biosystems, Foster City, CA) in the reflectron mode of operation. Data presented were typically HPLC analysis of a single experiment and converted using triplicate standard curves. Selected HPLC analyses were performed in duplicate or triplicate. The observed errors were within 10%.

Circular Dichroism. CD spectra of 3 μM AMCase in low-salt buffer [10 mM sodium citrate/citric acid, 20 mM sodium phosphate (pH 5.0), 0.005% Brij-35, and 1% DMSO] and high-salt buffer [10 mM sodium citrate/citric acid, 20 mM sodium phosphate (pH 5.0), 0.005% Brij-35, 1% DMSO, and 3.5 N sodium chloride] were recorded on a Jasco J-715 spectropolarimeter at 25 °C. The spectra were recorded over the range of 200−320 nm. Samples were scanned five times at a rate of 20 nm/min, and the spectra were averaged and curves smoothed. All experiments were repeated independently at least three times.

Intrinsic Tryptophan Fluorescence. The intrinsic tryptophan fluorescence of 3 μM AMCase was measured under the same buffer conditions that were used for CD experiments by exciting at 295 nm and measuring fluorescence emission from 320 to 460 nm. Control experiments were carried out by using a 100 μM *N*-acetyl-L-tryptophanamide solution under the same conditions. The fluorescence of 100 μM *N*-acetyl-L-tryptophanamide was comparable to that of 3 μM AMCase.

Analytical Ultracentrifugation. Sedimentation velocity experiments were performed on a Beckman XLI/XLA analytical ultracentrifuge, to investigate the effects of ionic strength on AMCase. AMCase (3 μM) in low-salt buffer [10 mM sodium citrate/citric acid and 20 mM sodium phosphate (pH 5.0)] and buffers containing various concentrations of NaCl [10 mM sodium citrate/citric acid, 20 mM sodium phosphate (pH 5.0), and 1, 2, or 3.5 N NaCl] was loaded into two-channel (1.2 cm path length) carbon-Epon centerpieces in an An-60 Ti titanium rotor. Scans were recorded at 20 °C with a rotor speed of 40 000 rpm, and the signal was detected at 280 nm with a spacing of 0.006 cm in the continuous mode. The sedimentation profiles were analyzed to obtain the distributions of the sedimentation coefficients using Sedfit (*19*). Samples were assayed for activity after AUC experiments (24 h later) and retained >90% of their original activities.

Size-Exclusion Chromatography and Multiangle Light Scattering. Size-exclusion chromatography (SEC) coupled with multiangle laser light scattering (MALLS) was used to obtain the molar mass of AMCase. The online light scattering measurements were performed on a Wyatt's DAWN EOS multiangle scattering laser photometer with a 25 mW GaAs (gallium arsenide) laser at 690 nm. The concentration of AMCase was monitored by either the absorbance or differential refractive index. The MALLS method yields a molar mass distribution and their moments [number-averaged mass (M_n), weight-averaged mass (M_w), and the *z*-averaged mass (M_z)], polydispersity, and the root-mean-square (rms) radius, r_g. The DNDC software was used to calculate the refractive

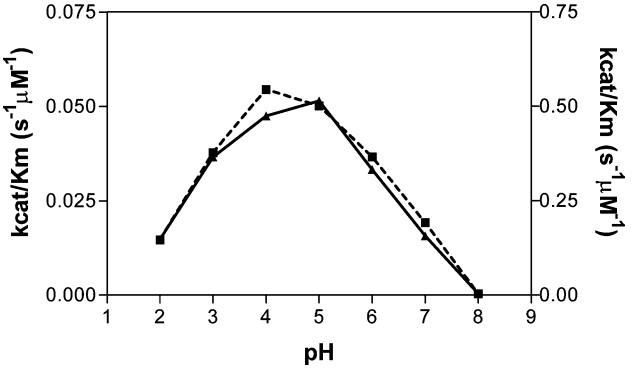

FIGURE 1: pH profile of human AMCase. The activity of AMCase was monitored by a fluorogenic assay from pH 2 to 9, using various concentrations of chitobiose-4MU (■, dashed line, left *y* axis) and chitotriose-4MU (▲, solid line, right *y* axis). Assays were performed in triplicate. The k_{cat}/K_m value was calculated as described in Materials and Methods.

index (RI) calibration constant. ASTRA software was used to process the light scattering data. AMCase was chromatographed on a Phenomenox Bio-Sep SEC4000 size-exclusion column with an Agilent 1100 instrument.

RESULTS

Enzyme Assay and pH Profile of Human AMCase. The chitinolytic activity of AMCase was assayed in a fluorogenic assay by using fluorogenic 4-methylumbelliferyl (4MU) chitooligosaccharide as substrate. The assay monitored continuously the fluorescence of 4MU generated from the specific cleavage of the β-glycosidic linkage between 4MU and GlcNAc. To determine the optimum assay pH, the chitinolytic activity of human AMCase was monitored by the fluorogenic assay from pH 2 to 10. Results indicate that there is one optimum pH around 4−5 for k_{cat}/K_m,[2] for chitobiose-4MU or chitotriose-4MU (Figure 1). No chitinolytic activity of human AMCase was detected at pH >8. A previous study has shown that mouse AMCase has a pH optimum around 2 and a secondary optimum around 3−6 using chitobiose-4MU as the substrate at a single concentration of 27 μM (*9*). For the rest of this report, assays were conducted at pH 5, unless specified otherwise.

Kinetic Mechanism of AMCase. The kinetic mechanism of AMCase was first examined using chitobiose-4MU as the substrate. The progress curves of 4MU formation with varied substrate concentrations were collected. Under normal assay conditions (1 nM AMCase), the progress curves were linear during the assay period (Figure 2A). The rate of 4MU formation was slower at substrate concentrations of 100 and 200 μM than at 50 μM, reflecting apparent substrate inhibition (Figure 2A,C). This observation is not due to the inner filter effect. In a separate control experiment, the fluorescence of 4MU was not quenched by chitobiose-4MU up to 400 μM. It is interesting to note that when the AMCase concentration was reduced to 0.25 nM, the progress curves of higher substrate concentrations, such as 100 and 200 μM, appeared biphasic (Figure 2B). These progress curves consisted of a fast phase within the initial several minutes, during which apparent substrate inhibition was absent,

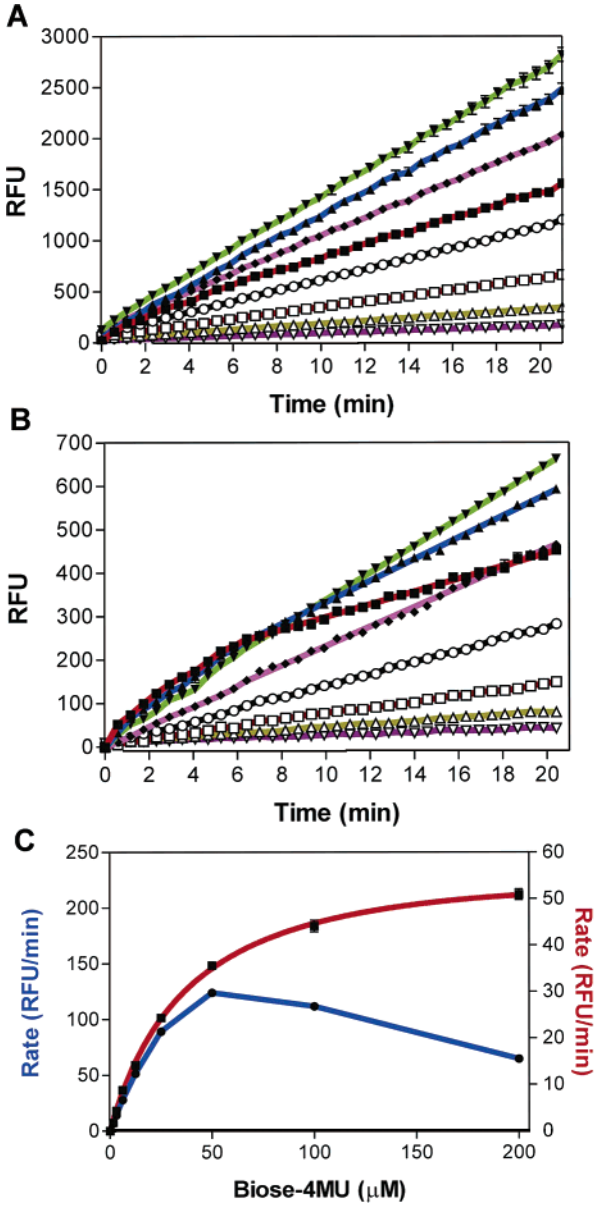

FIGURE 2: Progress curves of AMCase hydrolysis reactions. (A and B) Progress curves of the hydrolysis reaction of various concentrations of chitobiose-4MU [200 (■, red), 100 (▲, blue), 50 (▼, green), 25 (◆, purple), 12.5 (○, black), 6.25 (□, brown), 3.13 (△, olive), and 1.56 μM (▽, dark magenta)] by 1 and 0.25 nM AMCase, respectively. Assays were performed in triplicate. (C) Steady state rate plotted against the concentration of chitobiose-4MU: the rate within the first 20 min of plot A (●, blue, left *y* axis) and the rate within the first 3 min of plot B (■, red, right *y* axis; nonlinear regression to eq 1 generated a $K_{m,app}$ of 61 ± 1 μM and a k_{cat} of 0.81 ± 0.03 s^{-1}).

followed by a slower steady state phase. This result strongly suggests that apparent substrate inhibition is unlikely due to cooperative substrate binding or substrate inhibition. Instead, this deviation from the Michaelis−Menten behavior can be explained by an additional slow transglycosylation reaction as shown in Scheme 2. HPLC and mass spectrometry analysis confirmed the formation of chitotetraose-4MU, a transglycosylation product (experimental molecular mass of 989.2 Da, theoretical molecular mass of 989.0 Da).

In Scheme 2, biose-4MU binds to AMCase to form an ES complex and the cleavage of the β-glycosidic linkage between 4MU and GlcNAc releases 4MU (P_1). The nonco-

[2] Due to the apparent substrate inhibition, Michaelis−Menten analysis can provide accurate values of only k_{cat}/K_m.

Scheme 2: Kinetic Scheme of the AMCase Reaction

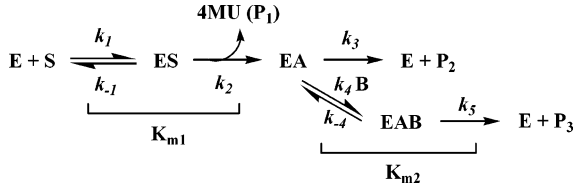

valent enzyme oxazolinium intermediate EA (also see Scheme 1) then partitions between hydrolysis to form product chitobiose (P_2) and transglycosylation reaction with a second molecule of substrate to produce transglycosylation product chitotetraose-4MU (P_3). The steady state rate equation of 4MU formation (P_1) derived from Scheme 2 is given by eq 2 (see the Supporting Information for details),

$$V_{P_1} = \frac{k_2 E_0}{1 + \frac{K_{m1}}{S} + \frac{k_2(B + K_{m2})}{k_5\left(B + \frac{k_3}{k_5}K_{m2}\right)}} \quad (2)$$

where K_{m1} and K_{m2} are intrinsic Michaelis constants, k_2, k_3, and k_5 are rate constants for products P_1, P_2, and P_3, respectively, E_0 is the enzyme concentration, S is the concentration of the first substrate, and B is the concentration of the second substrate for the transglycosylation reaction. In this reaction, the second substrate is the same as the first substrate. However, Scheme 2 and eq 2 can be applied to reactions in which the second substrate differs from the first substrate. In light of Scheme 2, the initial fast phase in Figure 2B approximately represents the presteady state preceding the slower transglycosylation reaction. Fitting of the average rate within 3 min to the Michaelis−Menten equation (eq 1) yielded a K_m value of 61 μM and a k_{cat} value of 0.81 s^{-1} (Figure 2C). These values may be slightly underestimated since the progress curves for higher substrate concentrations are not exactly linear within the initial 3 min. When $B = 0$ in Scheme 2, the model is reduced to the simple hydrolysis reaction free from the influence of transglycosylation reaction, as shown in eq 3. k_{cat} and K_m for this simple hydrolysis reaction are represented by eqs 4 and 5.

$$V_{P_1} = \frac{k_2 E_0}{1 + \frac{K_{m1}}{S} + \frac{k_2}{k_3}} \quad (3)$$

$$k_{catp_1} = k_2\frac{k_3}{k_2 + k_3} \quad (4)$$

$$K_{mP_1} = K_{m1}\frac{k_3}{k_2 + k_3} \quad (5)$$

Since the experimentally determined k_{cat} is 0.81 s^{-1}, this sets a lower limit of 0.81 s^{-1} for k_2 (eq 4). At this limiting k_2 value, K_{m1} would equal 61 μM. When the second substrate is saturating, eq 2 is simplified to eq 6:

$$V_{P_1} = \frac{k_2 E_0}{1 + \frac{K_{m1}}{S} + \frac{k_2}{k_5}} \quad (6)$$

Clearly, to have a reduced rate of 4MU formation due to transglycosylation, k_5 must be smaller than k_3. The maximal level of apparent inhibition is dependent on k_2/k_5: the higher the ratio, the higher the level of apparent inhibition.

To directly observe the transglycosidase activity of AMCase, chitohexaose and unhydrolyzable GlcNAc-4MU (see Indirect Transglycosylation Assay in Materials and Methods) were incubated with AMCase. Fluorescent 4MU product was indeed observed after a lag period (Figure 3A). Formation of 4MU confirms the transglycosidase activity of AMCase since 4MU can only come from the follow-up hydrolysis of transglycosylation products in this reaction. When unhydrolyzable chitotriose (see Indirect Transglycosylation Assay in Materials and Methods) and GlcNAc-4MU were incubated with AMCase, no reaction was observed (Figure 3A). Clearly, cleavage is a prerequisite step before transglycosylation.

Using unhydrolyzable substrate chitotriose as substrate B, the standard AMCase assay using chitobiose-4MU as the substrate was used to indirectly assess the transglycosylation reaction. It is assumed that by calculating the initial rate, the contribution from the secondary 4MU formation from AMCase hydrolysis of transglycosylation product chitotetraose-4MU is minimal. Figure 3B showed reactions of 6.25, 12.5, and 25 μM chitobiose-4MU and a varying concentration of chitotriose. Global fitting of the data into eq 2 by fixing K_{m1} at 61 μM gave the following: $k_2 = 0.75 \pm 0.01$ s^{-1} and $k_3K_{m2} = 5.6 \pm 1.0$ μM s^{-1}. This k_2 value is very close to the k_{cat} of 0.81 s^{-1}, consistent with the k_2 step being the rate-limiting step for hydrolysis. Chitinase-1 from *Coccidioides immitis*, another member of the family 18 chitinases, has also been reported to have a rate-limiting k_2 step (*20*). Assuming a k_3 of 3.8 s^{-1} ($5k_2$), K_{m2} is estimated to be 1.5 μM. The value of k_5 is near zero from global fitting, but individual fitting gave a rough estimate of $\sim 10^{-3}$ s^{-1}. The results are clearly consistent with the relation $k_5 \ll k_3$. Therefore, the apparent inhibition due to transglycosylation is because of the trapping of AMCase as the transglycosylation Michaelis complex (EAB).

Hydrolysis of GlcNAc Oligomers by AMCase. The anomeric forms of GlcNAc oligomer cleavage products from AMCase were determined by normal-phase HPLC, and the cleavage patterns were assessed from anomer formation. As shown in Figure 4, α and β forms of $(GlcNAc)_n$ have a 1:0.7 ratio for all GlcNAc oligomers at room temperature. Figure 4A shows major AMCase hydrolysis products from $(GlcNAc)_6$ are $(GlcNAc)_2$, $(GlcNAc)_3$, and $(GlcNAc)_4$. The two anomers of each product elute separately as a function of time. After reaction for 10 min, the α:β ratios of $(GlcNAc)_2$, $(GlcNAc)_3$, and $(GlcNAc)_4$ were ~1:3.2, ~1:1.6, and ~1:1, respectively; and the α:β ratio for the remaining $(GlcNAc)_6$ was 1:0.6. The results confirm the retaining mechanism of AMCase. To explain the α:β ratios of $(GlcNAc)_2$ and $(GlcNAc)_4$ products, AMCase must prefer the β anomer of $(GlcNAc)_6$ over the α anomer and must clip off $(GlcNAc)_2$ units from the nonreducing end. Correspondingly, to explain the α:β ratio of the $(GlcNAc)_3$ product, AMCase must also prefer the β anomer of $(GlcNAc)_6$ over the α anomer. The initial rate for cleavage between $(GlcNAc)_2$ and $(GlcNAc)_4$ is 3.9 s^{-1}, which is ~2-fold greater than the initial rate (2.0 s^{-1}) for cleavage between $(GlcNAc)_3$ and $(GlcNAc)_3$. Therefore, AMCase appears to recognize and cleave hexasaccharide

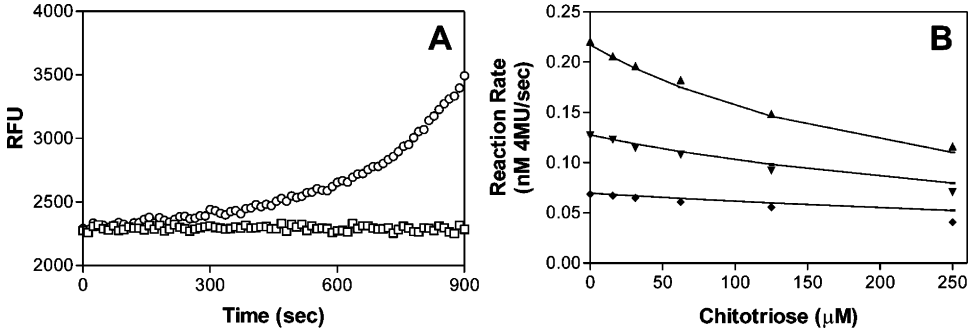

FIGURE 3: Transglycosylation reaction. (A) Progress curves of the hydrolysis reaction of the transglycosylation product from the mixture of 167 μM chitohexaose (○) or chitotriose (□) with 167 μM GlcNAc-4MU and 67 nM AMCase. (B) AMCase-catalyzed hydrolysis reactions at three chitobiose-4MU concentrations [25 (▲), 12.5 (▼), and 6.25 mM (◆)] in the presence of various chitotriose concentrations were monitored by the fluorogenic assay in triplicate.

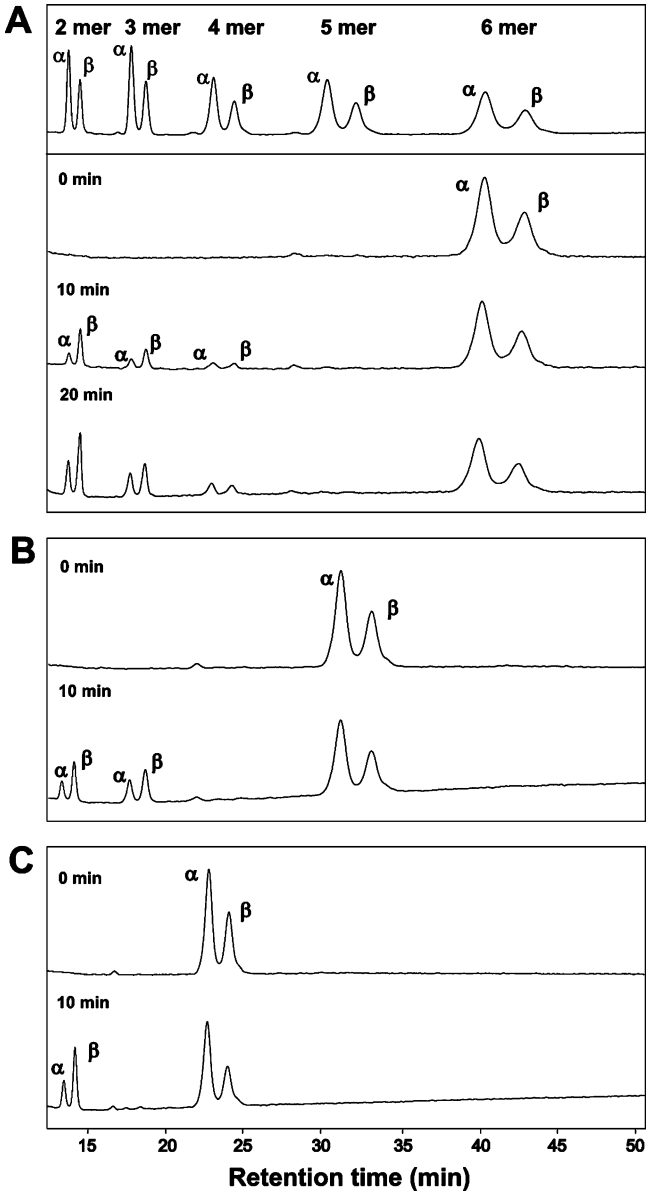

FIGURE 4: Hydrolysis of the GlcNAc oligomer by AMCase. HPLC analysis of the anomeric forms of the GlcNAc oligomer cleavage products from AMCase: GlcNAc oligomer standards and $(GlcNAc)_6$ (A), $(GlcNAc)_5$ (B), and $(GlcNAc)_4$ (C).

substrate from the nonreducing end primarily by disaccharide units and secondarily by trisaccharide units. Cleavage patterns of $(GlcNAc)_5$ and $(GlcNAc)_4$ are shown in panels

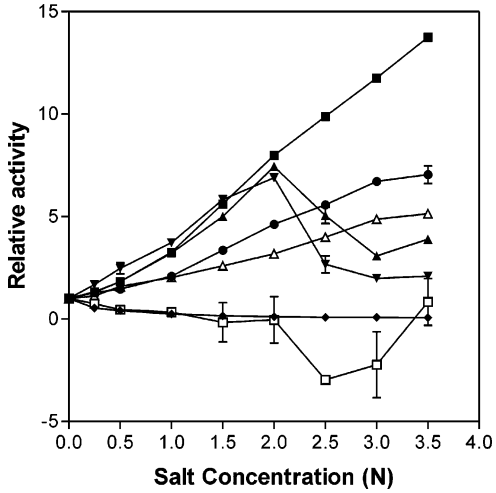

FIGURE 5: Effects of ionic strength on AMCase using chitobiose-4MU as the substrate. The chitinolytic activity of AMCase is monitored by the fluorogenic assay at 3.125 μM chitobiose-4MU in the presence of various concentrations of anionic sodium salts: NaCl (■), Na_2SO_4 (▲), NaP_i (▼), NaOAc (◆), NaBr (●), NaI (□), and Na citrate (△) buffers. The average of three experiments is plotted.

B and C of Figure 4, and data also suggest that AMCase prefers the β anomer of $(GlcNAc)_{4-5}$ as a substrate and recognizes and hydrolyzes chitooligosaccharides from the nonreducing end primarily via a disaccharide.

Ionic Strength Effects. Effects of ionic strength on the chitinolytic activity of AMCase were assessed by both a fluorogenic assay using chitobiose-4MU and chitotriose-4MU as substrate and a HPLC assay using chitooligosaccharide as substrate. When chitobiose-4MU was used as substrate, we observed that AMCase activity increased in the presence of high salt concentrations, and the magnitude of this effect is dependent on the nature of the anion (Figure 5). AMCase is ~15-fold more active in the presence of 3.5 N NaCl. The overall anion effect follows the Hofmeister series when the salt concentrations are less than 2 N, except for citrate: sulfate > phosphate > chloride > bromide > citrate > acetate > iodide (*21*). The weaker effect of citrate that usually sits on the top of Hofmeister series is likely due to partial ionization at our experimental pH of 5. When the salt concentration is higher than 2.0 N, the relative activities of AMCase decreased for sulfate and phosphate series. We speculate that this abnormal behavior is due to anion/water clusters formed at high sulfate or phosphate concentrations. The effect of cation is dependent on anionic partners, and

Table 1: Initial Rates of Substrate Disappearance and Product Formation[a] from Hydrolysis of Fluorogenic Substrates by AMCase at Three Substrate Concentrations under Low- and High-Ionic Strength Conditions

	substrate concentration (μM)	ionic strength[b]	initial rate				
			chitotriose-4MU	chitobiose-4MU	GlcNAc-4MU	4MU	transglycosylation[c]
chitotriose-4MU	3.1	low	−2.66	0	2.02	0.64	0
		high	−6.93	0	1.62	5.37	0
	50	low	−7.69	0.14	5.51	1.21	0.82
		high	−9.92	0	1.57	4.86	3.48
	100	low	−3.66	0	2.63	0.67	0.36
		high	−4.32	0	0.83	2.66	0.84
chitobiose-4MU	3.1	low	0	−0.07	0	0.07	0
		high	0	−0.75	0	0.75	0.09
	50	low	0	−1.08	0.13	0.81	0.25
		high	0	−3.65	0	3.05	0.65
	100	low	0.0003[c]	−1.35	0.12	0.82	0.55[d]
		high	0.02[c]	−4.6	0	2.79	1.57[d]

[a] Initial rate within 10 min (nanomolar per second). [b] Low-salt buffer: 10 mM sodium citrate/citric acid, 20 mM sodium phosphate (pH 5.0), 0.005% Brij-35, and 1% DMSO. High-salt buffer: 3.5 N NaCl, 10 mM sodium citrate/citric acid, 20 mM sodium phosphate (pH 5.0), 0.005% Brij-35, and 1% DMSO. [c] Since most transglycosylation products appeared after 40 min, the average rates were used here. [d] Including chitotriose-4MU.

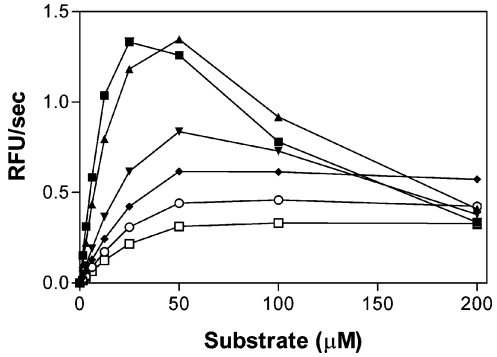

FIGURE 6: Chitobiose-4MU dose titrations at various salt concentrations. The steady state rate plotted against the concentration of chitobiose-4MU at various NaCl concentrations of 3 (■), 2 (▲), 1 (▼), 0.5 (◆), 0.25 (○), and 0 N (□). Assays were performed in triplicate.

sodium chloride elevates the activity of AMCase more significantly than other chloride salts that were tested (data not shown).

Ionic strength effects were also monitored at different chitobiose-4MU concentrations at various NaCl concentrations (Figure 6). At higher salt concentrations, the activity of AMCase increased considerably as expected; however, apparent substrate inhibition was also more significant under higher-salt conditions. As we have shown earlier, the maximal level of apparent inhibition depends on the k_2/k_5 ratio (Scheme 2). In the presence of a high level of salt, the rate of 4MU formation is significantly enhanced at lower substrate concentrations (Figure 6). As discussed previously, k_2 is most likely the rate-limiting step under normal assay conditions. Thus, k_2 must also be significantly enhanced under high-salt conditions. Separate HPLC analysis (Table 1) confirmed that high salt significantly enhances the rate of 4MU formation and showed that high salt slightly increases the rate of the transglycosylation reaction. Thus, the overall k_2/k_5 ratio is increased under high-salt conditions, which explains corresponding higher-level apparent substrate inhibition under high-salt conditions.

When chitotriose-4MU was used as a substrate, we also observed a similar enhanced rate of 4MU formation in high-salt environments. However, HPLC analysis of chitotriose-4MU revealed a more complex story. Figure 7 shows an example of time course HPLC analysis of chitotriose-4MU hydrolysis by AMCase at low and high salt concentrations. Detailed results of initial rates of substrate hydrolysis and product formation are listed in Table 1. Under low-salt conditions, the major site of cleavage of chitotriose-4MU by AMCase is the β-1,4-glycosidic linkage between the second and third GlcNAc from the nonreduction end (Figure 7A and Table 1). The rate of this cleavage is ~3−4-fold faster than the cleavage occurring between GlcNAc and 4MU. However, high-salt conditions both enhance the rate of cleavage between GlcNAc and 4MU and decrease the rate of the cleavage between the second and third GlcNAc such that the major cleavage site is switched to that between GlcNAc and 4MU (Figure 7B and Table 1). For both chitobiose-4MU and chitotriose-4MU substrates, we also observed minor but detectable reaction that removes one GlcNac from the nonreducing end under certain conditions (Table 1).

We next examined possible effects of ionic strength on AMCase-catalyzed cleavage of natural chitooligosaccharides $(GlcNAc)_{4-6}$ using normal-phase HPLC. Our results showed that reaction rates of chitooligosaccharides were also enhanced by higher ionic strengths (Figure 8). In the presence of 1.5 N NaCl, the rates of cleavage of chitopentaose and chitotetraose by AMCase increased ~3-fold while the cleavage rate for chitohexaose increased 7-fold. Apparent substrate inhibition was also observed at chitooligosaccharide concentrations higher than 100 μM (data not shown), and the salt effect was not observed at chitooligosaccharide concentrations higher than 200 μM. Unlike fluorogenic substrates chtiobiose-4MU and chitotriose-4MU, no change in the cleavage pattern of chitooligosaccharides was observed.

Biophysical Properties of AMCase under High-Salt Conditions. Biophysical methods were applied to elucidate possible changes in the structure of AMCase under high-salt conditions. Circular dichroism results between 200 and 320 nm revealed no significant secondary structural changes between low- and high-salt conditions (data not shown). No significant structural changes were detected by the intrinsic tryptophan fluorescence method. The tryptophan fluorescence was essentially the same under low- and high-salt conditions (data not shown). Sedimentation velocity experiments showed that the monomeric AMCase migrates with a sedimentation

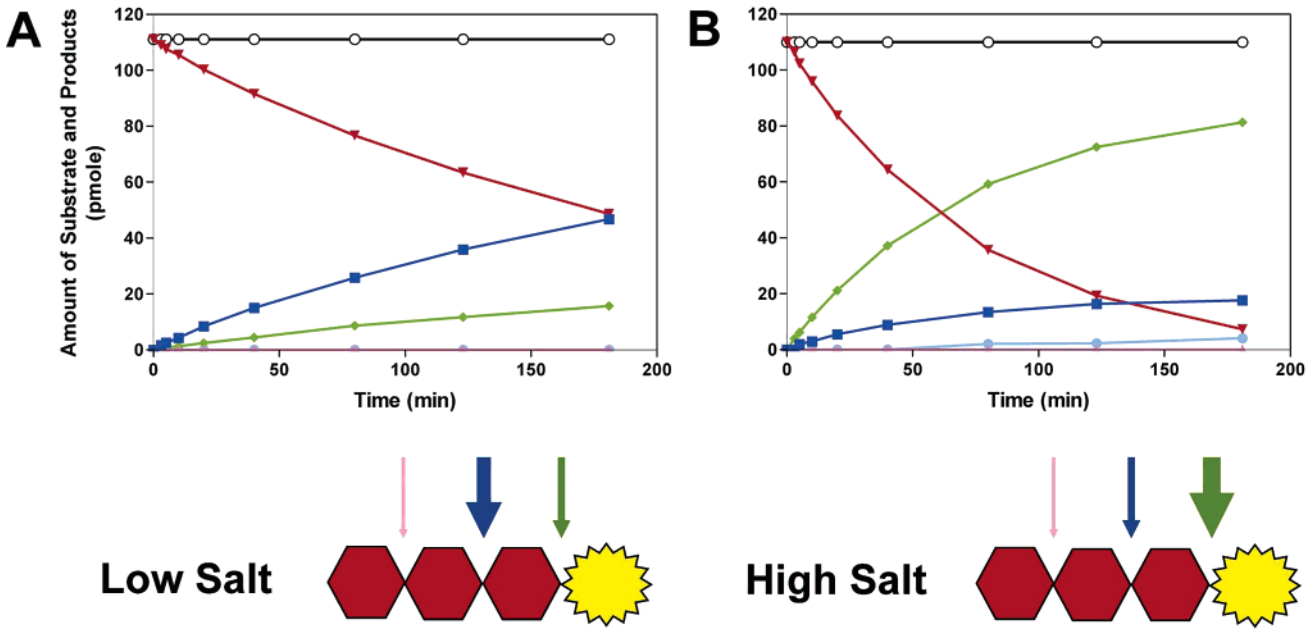

FIGURE 7: Effects of ionic strength on AMCase using chitotriose-4MU as the substrate. HPLC time course plots of 110 μM chitotriose-4MU hydrolyzed by 1 nM AMCase under (A) low-salt (0 N NaCl) and (B) high-salt (3.5 N NaCl) conditions: total (○), chitotriose-4MU (▼, red), chitobiose-4MU (▲, pink), GlcNAc-4MU (■, blue), 4MU (◆, green), and transglycosylation (●, ice blue).

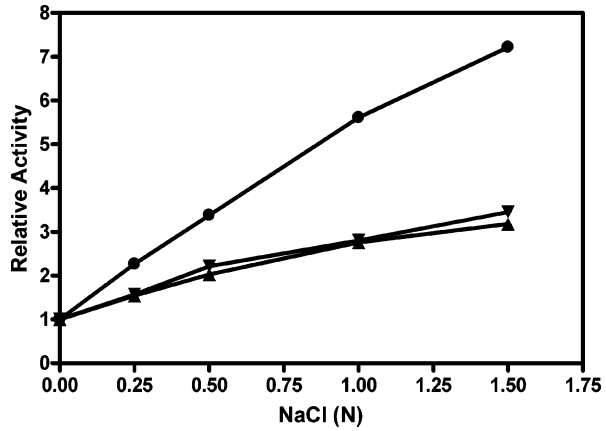

FIGURE 8: Effects of ionic strength on AMCase using chitooligosaccharides as the substrate. Steady state rate of chitotetraose (▼), chitopentaose (▲), and chitohexaose (●) plotted against the concentration of NaCl.

coefficient of ca. 4.0 S (~50 kDa) at all tested concentrations of NaCl (0, 1, 2, and 3.5 N). The SEC−MALLS experiment under low-salt conditions confirmed the monomeric state of AMCase (data not shown). Attempts to acquire SEC−MALLS data under high-salt conditions were not successful. Overall, these results suggest that ionic strength does not promote AMCase oligomerization and does not alter the global structure of AMCase.

DISCUSSION

AMCase is one of the critical proteins that are involved in Th2-mediated inflammation. Even though the physiological substrate(s) of AMCase in human and the exact mechanism by which AMCase regulates Th2-driven inflammation are still unknown, this enzyme is rapidly emerging as a novel therapeutic target in the area of asthma and allergic diseases. This study attempts to gain further insight into the kinetic mechanism of human AMCase. Detailed knowledge of AMCase mechanism may help the identification of the endogenous substrate(s) of AMCase, the design of specific and potent inhibitors of AMCase, and the elucidation of the mechanism of the involvement of AMCase in inflammation.

Human AMCase is a member of the family 18 glycosyl hydrolases and thus is expected to follow the substrate-assisted catalytic mechanism as shown in Scheme 1. During initial kinetic characterization of human AMCase, we observed apparent substrate inhibition of the enzyme in a fluorogenic assay (Figure 2A,B). Several simple mechanisms that may explain this deviation from the Michaelis−Menten model include the inner filter effect, cooperativity of substrate binding, and substrate inhibition. We showed that the fluorescence of the 4MU product is not quenched by the substrate, thus ruling out the inner filter effect. Hence, the simple hydrolysis reaction as shown in Scheme 1 cannot adequately explain the results in Figure 2A. At a reduced AMCase concentration, we observed biphasic progress curves at higher substrate concentrations (Figure 2B). The fact that apparent substrate inhibition was not present during the initial phase (Figure 2B,C) suggests the observed kinetics is not due to cooperativity of substrate binding or substrate inhibition. We propose an additional "slow" transglycosylation step in the AMCase reaction as shown in Scheme 2. This model can now fully account for progress curves in panels A and B of Figure 2 if k_5 is slower than k_3. Indeed, the transglycosidase activity was directly observed when chitohexaose and unhydrolyzable GlcNAc-4MU were incubated with AMCase (Figure 3A). We next applied unhydrolyzable chitotriose as the second substrate for transglycosylation. Fitting of data to steady state eq 2 provided an estimate of 10^{-3} s^{-1} for k_5, confirming $k_5 \ll k_3$. Equation 2 also dictates the maximal level of apparent inhibition is dependent on the k_2/k_5 ratio. This prediction has been validated by assay results from various experimental conditions (ionic strength and pH). We observed that a higher ionic strength leads to a higher level of apparent substrate inhibition, while a lower pH (pH data not shown) leads to weaker inhibition. In both cases,

the level of inhibition can be adequately explained by an increase or decrease in the k_2/k_5 ratio. In addition, the estimate of K_{m2} for transglycosylation is more than 1 order of magnitude lower than the K_{m1} for hydrolysis. This implies that the transglycosylation reaction of AMCase may provide negative feedback regulation in vivo of the chitinase reaction of AMCase. We speculate that the negative feedback regulation might help explain the so-called hygiene hypothesis (*22*). It has been shown that only chitin of a certain size (1−20 μm) is able to decrease serum IgE levels and lung eosinophilia (*23*) and to downregulate symptoms of allergic hypersensitivity in mouse models of allergy (*24*). Clearly, further investigation of yet-to-be identified endogenous substrates of AMCase would help to elucidate this complicated inflammatory mechanism.

Apparent substrate inhibition has been reported in many chitinase systems (*20*, *25*, *26*). There have been generally two types of explanations in the literature. Some have been tentatively attributed to complex substrate inhibition due to the binding of multiple substrate molecules (*20*, *25*), while others have been attributed to transglycosylation (*26*). In the case of human chitotriosidase where transglycosylation was observed with chitobiose-4MU, the kinetics reverted back to normal Michaelis−Menten behavior when 4MU-(4-deoxy)chitobiose, a nonacceptor for transglycosylation, was used as the substrate (*26*). Therefore, the futile cleavage of transglycosylation products was proposed to account for the apparent substrate inhibition (*26*). In our opinion, this explanation of how the transglycosidase activity of chitotriosidase results in apparent substrate inhibition is not sufficient. Because all kinetic data in this chitotriosidase paper were measuring initial velocities, negligible amounts of transglycosylation products cannot be the main factor. On the basis of our model, the slow transglycosylation step should also be responsible for apparent substrate inhibition in the case of chitotriosidase. For chitinase-1 from *Coccidioides immitis* (CiX1) in which transglycosylation was observed, the data simulation showed the rate of transglycosylation is faster than the rate of hydrolysis (*20*). According to eq 2 derived in our study, transglycosylation cannot be the major factor for apparent substrate inhibition in CiX1, consistent with the authors' proposal of complex substrate inhibition due to multiple-substrate binding. In all previous published examples, transglycosylation has not been quantitatively characterized.

Family 18 chitinases cleave the β-1,4-glycosidic bond to produce the β anomer as a product through the retaining mechanism. HPLC analysis of $(GlcNAc)_{4-6}$ confirms that hydrolysis products of AMCase are β anomers. Surprisingly, AMCase also prefers the β form of chitooligosaccharide as a substrate. This preference of the β form of the substrate and the formation of the β anomer product may be features that could be utilized in the design of substrate mimics as inhibitors of AMCase. On the basis of hydrolysis of $(GlcNAc)_{4-6}$, AMCase appears to recognize and cleave chitooligosaccharide substrates from the nonreducing end primarily by disaccharide units and secondarily by trisaccharide units. Boot et al. (*9*) reported that mouse AMCase cleaves colloidal chitin to generate $(GlcNAc)_2$ as the only product. Therefore, AMCase may function as an exo-chitobiosidase, and to a lesser extent as a chitotriosidase. The more definitive classification of AMCase awaits additional HPLC experiments with longer length chitooligosaccharides. For human chitotriosidase whose sequence is 57% identical with that of human AMCase, while published experimental data do not conclusively support classification of chitotriosidase as an endo- or exo-chitinase, the enzyme has been suggested to be an endo-chitinase based upon its X-ray crystal structure (*27*). The primary amino acid sequence of human AMCase shows the presence of two more conserved cysteine residues in the catalytic core than in human chitotriosidase. If the classification of AMCase and chitotriosidase holds, this diversification may be attributed to differences between their substrate binding domains and/or conformational dynamics that are constrained by the extra disulfide bond in AMCase.

Enhancement of chitinolytic activity of human AMCase against chitobiose-4MU and chitotriose-4MU was observed under higher-ionic strength conditions. This activation is highly anion-dependent and appears to follow the Hofmeister series. The effect of the cation was less pronounced and dependent on anionic partners under our assay conditions. HPLC analysis reveals that salt alters the cleavage pattern against chitotriose-4MU such that AMCase behaves primarily as a chitotriosidase under high-salt conditions while primarily as a chitobiosidase under low-salt conditions. Changes in the substrate cleavage pattern also suggest that the effects of ionic strength are unlikely due to nonspecific salting-out of the substrate. Under high-salt conditions, the chitinolytic activities of AMCase against natural chitooligosaccharides were also enhanced when the concentrations of substrates were lower than 200 μM. At high substrate concentrations, the observed rates were complicated by apparent substrate inhibition due to transglycosylation and no salt effect was observed.

Characterization of AMCase by various biophysical methods suggests that high salt does not alter the global structure of AMCase. However, the enhanced catalytic activity and altered cleavage pattern of chitotriose-4MU under high-salt conditions must imply localized conformational changes around the active site of AMCase. The observed in vitro salt effects of AMCase could have physiological implications in vivo. AMCase is an important downstream Th2 effector of cytokine IL-13-mediated inflammation pathway (*13*). Allergic airway inflammation could affect the absorption and secretion of electrolytes across the apical and basolateral membranes through ion (Na^+, K^+, and Cl^-) selective channels (*28*). Several lines of evidence have already indicated that cytokines IL-13 and IL-4 regulate epithelial electrolyte transport (*15*, *16*, *29*). Thus, AMCase activity in vivo may be modulated by ionic strength.

Although fluorogenic substrates chitotriose-4MU and chitobiose-4MU have been widely used for chitinase studies, salt-regulated chitinase activity against fluorogenic substrates identified in this study indicates that maintaining a constant salt concentration is crucial in meaningfully comparing chitinase activities under two sets of conditions. This fact has largely been ignored in the literature studies of chitinases. Only limited studies have reported the effects of ionic strength on chitinase. The chitin-binding domain of chitinase A1 from *Bacillus circulans* has enhanced chitin binding activity in the presence of 0.5 M NaCl (*30*), and one mutation of this protein has been shown to reduce its chitin binding activity in the presence of 0−1.0 M NaCl but allows strong

binding to chitin at 2.0 M NaCl (*31*). Another study shows that chitinase B from *Microbulbifer degradans* has no significant changes in chitinolytic activity against fluorogenic substrates at 1.0 M NaCl (*32*). These observations indicate that ionic strength may have differential effects on different chitinases, although they all share the same conserved catalytic motif (DXXDXDXE).

Both fluorogenic assays and HPLC analysis (data now shown) indicate that the chitinolytic activity of human AMCase has one optimum pH for k_{cat}/K_m around 4−5. A previous study of mouse AMCase reported a distinct major pH optimum around 2, in addition to a pH optimum between 3 and 6 (*9*). Human AMCase is strongly expressed in stomach and at a lower level in the lung. Even though the physiological substrates of human AMCase are not known, it is generally believed that the stomach AMCase functions as a food processor (*9*). A pH optimum of 4−5 casts some doubt on human AMCase's primary role as a chitin hydrolase in the stomach. On the other hand, the fact that fluid condensed from the breath of patients with acute asthma is acidic (pH ∼5.2) and fluid from the breath of normal men is slight basic (pH ∼7.7) (*17*) underscores the possible physiological relevance of an optimum pH around 4−5 for chitinolytic activity of human AMCase in the lung. Results from HPLC analysis also indicate that transglycosidase activity of human AMCase is higher at pH 2 than at pH 5 and 7 (data not shown), suggesting that the transglycosylation reaction may have a lower pH optimum than the hydrolysis reaction. Since transglycosylation and hydrolysis are generally expected to use the same catalytic machinery of the enzyme, we do not understand currently distinct pH optima for the two reactions. As discussed earlier, the transglycosylation reaction can account for the observed apparent substrate inhibition of the hydrolysis reaction and possibly provides the feedback regulation of the hydrolysis reaction. The distinct pH optima of transglycosylation and hydrolysis thus may add another layer of regulation of human AMCase activity.

In summary, this report presents the first detailed kinetic characterization of human AMCase. We showed that a slow transglycosylation step in the AMCase reaction leads to the observation of apparent substrate inhibition and may provide feedback regulation of AMCase in vivo. We demonstrated that AMCase prefers the β anomer of chitooligosaccharides and mainly functions as an exo-chitobiosidase. Our results reveal that AMCase experiences elevated chitinolytic activity in a high-ionic strength environment. The pH optimum of human AMCase is consistent with possible roles in lung inflammation. The studies reported here provide a springboard for further elucidating the mechanism of involvement of AMCase in inflammation and developing more specific and potent inhibitors of AMCase that may be utilized in treatment of asthma and other allergic diseases.

ACKNOWLEDGMENT

We thank Bhupesh Kapoor and Keiko Tabei for assistance with analytical ultracentrifugation and the mass spectrometer, respectively.

SUPPORTING INFORMATION AVAILABLE

Detailed derivation of eq 2 from Scheme 2. This material is available free of charge via the Internet at http://pubs.acs.org.

REFERENCES

1. Cohen-Kupiec, R., and Chet, I. (1998) The molecular biology of chitin digestion, *Curr. Opin. Biotechnol. 9*, 270−7.
2. Henrissat, B., and Bairoch, A. (1993) New families in the classification of glycosyl hydrolases based on amino acid sequence similarities, *Biochem. J. 293*, 781−8.
3. Tews, I., Terwisscha van Scheltinga, A. C., Perrakis, A., Wilson, K. S., and Dijkstra, B. W. (1997) Substrate-Assisted Catalysis Unifies Two Families of Chitinolytic Enzymes, *J. Am. Chem. Soc. 119*, 7954−9.
4. Brameld, K. A., Shrader, W. D., Imperiali, B., and Goddard, W. A., III (1998) Substrate assistance in the mechanism of family 18 chitinases: Theoretical studies of potential intermediates and inhibitors, *J. Mol. Biol. 280*, 913−23.
5. van der Holst, P. P. G., Schlaman, H. R. M., and Spaink, H. P. (2001) Proteins involved in the production and perception of oligosaccharides in relation to plant and animal development, *Curr. Opin. Struct. Biol. 11*, 608−16.
6. Hart, P. J., Pfluger, H. D., Monzingo, A. F., Hollis, T., and Robertus, J. D. (1995) The refined crystal structure of an endochitinase from *Hordeum vulgare* L. seeds at 1.8 Å resolution, *J. Mol. Biol. 248*, 402−13.
7. Garcia-Casado, G., Collada, C., Allona, I., Casado, R., Pacios, L. F., Aragoncillo, C., and Gomez, L. (1998) Site-directed mutagenesis of active site residues in a class I endochitinase from chestnut seeds, *Glycobiology 8*, 1021−8.
8. Boot, R. G., Renkema, G. H., Strijland, A., van Zonneveld, A. J., and Aerts, J. M. (1995) Cloning of a cDNA encoding chitotriosidase, a human chitinase produced by macrophages, *J. Biol. Chem. 270*, 26252−6.
9. Boot, R. G., Blommaart, E. F. C., Swart, E., Ghauharali-van der Vlugt, K., Bijl, N., Moe, C., Place, A., and Aerts, J. M. F. G. (2001) Identification of a Novel Acidic Mammalian Chitinase Distinct from Chitotriosidase, *J. Biol. Chem. 276*, 6770−8.
10. Hollak, C. E., van Weely, S., van Oers, M. H., and Aerts, J. M. (1994) Marked elevation of plasma chitotriosidase activity. A novel hallmark of Gaucher disease, *J. Clin. Invest. 93*, 1288−92.
11. Rao, F. V., Houston, D. R., Boot, R. G., Aerts, J. M. F. G., Sakuda, S., and Van Aalten, D. M. F. (2003) Crystal Structures of Allosamidin Derivatives in Complex with Human Macrophage Chitinase, *J. Biol. Chem. 278*, 20110−6.
12. Renkema, G. H., Boot, R. G., Strijland, A., Donker-Koopman, W. E., van den Berg, M., Muijsers, A. O., and Aerts, J. M. (1997) Synthesis, sorting, and processing into distinct isoforms of human macrophage chitotriosidase, *Eur. J. Biochem. 244*, 279−85.
13. Zhu, Z., Zheng, T., Homer, R. J., Kim, Y.-K., Chen, N. Y., Cohn, L., Hamid, Q., and Elias, J. A. (2004) Acidic Mammalian Chitinase in Asthmatic Th2 Inflammation and IL-13 Pathway Activation, *Science 304*, 1678−82.
14. Elias, J. A., Homer, R. J., Hamid, Q., and Lee, C. G. (2005) Chitinase and chitinase-like proteins in Th2 inflammation and asthma, *J. Allergy Clin. Immunol. 116*, 497−500.
15. Danahay, H., Atherton, H., Jones, G., Bridges, R. J., and Poll, C. T. (2002) Interleukin-13 induces a hypersecretory ion transport phenotype in human bronchial epithelial cells, *Am. J. Physiol. 282*, L226−36.
16. Galietta, L. J. V., Pagesy, P., Folli, C., Caci, E., Romio, L., Costes, B., Nicolis, E., Cabrini, G., Goossens, M., Ravazzolo, R., and Zegarra-Moran, O. (2002) IL-4 is a potent modulator of ion transport in the human bronchial epithelium in vitro, *J. Immunol. 168*, 839−45.
17. Hunt, J. F., Fang, K., Malik, R., Snyder, A., Malhotra, N., Platts-Mills, T. A. E., and Gaston, B. (2000) Endogenous Airway Acidification. Implications for Asthma Pathophysiology, *Am. J. Respir. Crit. Care Med. 161*, 694−9.
18. Koga, D., Yoshioka, T., and Arakane, Y. (1998) HPLC analysis of anomeric formation and cleavage pattern by chitinolytic enzyme, *Biosci., Biotechnol., Biochem. 62*, 1643−6.
19. Schuck, P. (2000) Size distribution analysis of macromolecules by sedimentation velocity ultracentrifugation and Lamm equation modeling, *Biophys. J. 78*, 1606−19.
20. Fukamizo, T., Sasaki, C., Schelp, E., Bortone, K., and Robertus, J. D. (2001) Kinetic Properties fo Chitinase-1 from the Fungal Pathogen *Coccidioides immitis*, *Biochemistry 40*, 2448−54.

21. Hofmeister, F. (1888) Zur Lehre der wirkung der salze. Zweite mittheilung, *Arch. Exp. Pathol. Pharmakol. 24*, 247−60.
22. Strachan, D. (1989) Hay fever, hygiene, and household size, *BMJ [Br. Med. J.] 299*, 1259−60.
23. Shibata, Y., Foster, L. A., Bradfield, J. F., and Myrvik, Q. N. (2000) Oral Administration of Chitin Down-Regulates Serum IgE Levels and Lung Eosinophilia in the Allergic Mouse, *J. Immunol. 164*, 1314−21.
24. Strong, P., Clark, H., and Reid, K. (2002) Intranasal application of chitin microparticles down-regulates symptoms of allergic hypersensitivity to *Dermatophagoides pteronyssinus* and *Aspergillus fumigatus* in murine models of allergy, *Clin. Exp. Allergy 32*, 1794−800.
25. Honda, Y., Kitaoka, M., Tokuyashu, K., Sasaki, C., Fukamizo, T., and Hayashi, K. (2003) Kinetic Studies on the Hydrolysis of N-Acetylated and N-Deacetylated Derivatives of 4-Methylumbelliferyl Chitobioside by the Family 18 Chitinases ChiA and ChiB from *Serratia marcesscens*, *J. Biochem. 133*, 253−8.
26. Aguilera, B., Ghauharali-van der Vlugt, K., Helmond, M. T. J., Out, J. M. M., Donker-Koopman, W. E., Groener, J. E. M., Boot, R. G., Renkema, G. H., van der Marel, G. A., van Boom, J. H., Overkleeft, H. S., and Aerts, J. M. F. G. (2003) Transglycosidase Activity of Chitotriosidase: IMPROVED ENZYMATIC ASSAY FOR THE HUMAN MACROPHAGE CHITINASE, *J. Biol. Chem. 278*, 40911−6.
27. Fusetti, F., von Moeller, H., Houston, D., Rozeboom, H. J., Dijkstra, B. W., Boot, R. G., Aerts, J. M., and van Aalten, D. M. (2002) Structure of human chitotriosidase. Implications for specific inhibitor design and function of mammalian chitinase-like lectins, *J. Biol. Chem. 277*, 25537−44.
28. Cloutier, M. M., Guernsey, L., Wu, C. A., and Thrall, R. S. (2004) Electrophysiological properties of the airway, *Am. J. Pathol. 164*, 1849−56.
29. Zünd, G., Madara, J. L., Dzus, A. L., Awtrey, C. S., and Colgan, S. P. (1996) Interleukin-4 and Interleukin-13 Differentially Regulate Epithelial Chloride Secretion, *J. Biol. Chem. 271*, 7460−4.
30. Hashimoto, M., Ikegami, T., Seino, S., Ohuchi, N., Fukada, H., Sugiyama, J., Shirakawa, M., and Watanabe, T. (2000) Expression and characterization of the chitin-binding domain of Chitinase A1 from *Bacillus circulans* WL-12, *J. Bacteriol. 182*, 3045−54.
31. Ferrandon, S., Sterzenbach, T., Mersha, F. B., and Xu, M.-Q. (2003) A single surface tryptophan in the chitin-binding domain from *Bacillus circulans* chitinase A1 plays a pivotal role in binding chitin and can be modified to create an elutable affinity tag, *Biochim. Biophys. Acta 1621*, 31−40.
32. Howard, M. B., Ekborg, N. A., Taylor, L. E. I., Weiner, R. M., and Hutcheson, S. W. (2004) Chitinase B of "*Microbulbifer degradans*" 2−40 contains two catalytic domains with different chitinolytic activities, *J. Bacteriol. 186*, 1297−303.

BI0525977